Galactosylated α,β-poly[(2-hydroxyethyl)-L-aspartamide]-bound doxorubicin: improved antitumor activity against hepatocellular carcinoma with reduced hepatotoxicity

Xiaoyun Cheng[a,b], Fengbo Gao[a], Jiawei Xiang[a], Xiqun Jiang[b,d], Jiangning Chen[a,c] and Junfeng Zhang[a,c,d]

Galactosyl-terminated drug carriers are known to enhance drug accumulation in the liver, while possible accompanying hepatic toxicity is usually not clarified. This study developed a galactosyl–α,β-poly[(2-hydroxyethyl)-L-aspartamide]–doxorubicin conjugate (Gal–PHEA–DOX) and investigated its therapeutic efficacy and safety in orthotopic hepatocellular carcinoma-bearing mice. Gal–PHEA–DOX had a galactosylation degree of 7.5 mol% and a DOX content of 8.9 wt%. A biodistribution study showed that Gal–PHEA–DOX sustainedly circulated in the plasma and highly accumulated in hepatocarcinoma. Free drug liberated from Gal–PHEA–DOX was relatively low in the liver and heart as compared with that of the DOX administration. The Gal–PHEA–DOX conjugate showed superior cytotoxicity against the hepatocellular carcinoma cell line HepG2 as compared with the nongalactosylated PHEA–DOX conjugate. Gal–PHEA–DOX exhibited comparable antitumor activity with PHEA–DOX in the S180-bearing mice, but more effective than PHEA–DOX or DOX in the Heps-bearing mice with negligible detrimental effect in the liver remnant. A systemic toxicity study showed that this conjugate did not show either cytotoxicity or hepatotoxicity at a relatively high dose, which would be harmful for free DOX. These results suggest that the Gal–PHEA–DOX conjugate has great potential for use in hepatocellular carcinoma chemotherapy because of its enhanced antitumor effect with reduced systemic toxicity including hepatotoxicity.

Anti-Cancer Drugs 2011, **22**:136–147

Keywords: α, β-poly[(2-hydroxyethyl)-L-aspartamide], doxorubicin, galactosyl, hepatocellular carcinoma, hepatotoxicity

[a]State Key Laboratory of Pharmaceutical Biotechnology, School of Life Sciences, [b]Laboratory of Mesoscopic Chemistry and Department of Polymer Science and Engineering, College of Chemistry and Chemical Engineering, [c]Jiangsu Provincial Diabetes Center and [d]Jiangsu Provincial Laboratory for Nano-Technology, Nanjing University, Nanjing, China

Correspondence to Junfeng Zhang, PhD, and Jiangning Chen, PhD, Nanjing University, 22 Hankou Road, Nanjing 210093, China
Tel: +86 25 83593562, +86 25 83596796; fax: +86 25 83324605;
e-mail: jfzhang@nju.edu.cn; jnchen@nju.edu.cn

Received 12 May 2010 **Revised form accepted** 10 September 2010

Introduction

Hepatocellular carcinoma (HCC) is the most common primary malignant tumor of the liver in non-Western countries. Doxorubicin (DOX) is an anthracyclic antibiotic that shows broad-spectrum activity for solid tumors and has been tried in HCC chemotherapy since 1975 [1,2]. However, DOX has always been reported to have limited activity at conventional doses because HCC is poorly responsive to chemotherapy by expressing the multidrug resistance gene and consequent high levels of permeability-glycoprotein [3]. Dose escalation of DOX is hindered by the unacceptable levels of toxicity in these patients with impaired hepatic function [4]. To improve the therapeutic efficacy of DOX in HCC, target strategies have been used to modify the drug. The galactosyl (Gal) group is a frequently used ligand for facilitating liver targeting. It can bind to the asialoglycoprotein receptor (ASGP-R), which is highly expressed on the cell plasma membrane in all the cells of the majority of well-differentiated HCCs, including the proliferating ones [5]. To restrict the action of DOX in the liver and reduce its extrahepatic toxicity, DOX has been delivered by some Gal-terminating carriers such as N-(2-hydroxypropyl)-methacrylamide copolymers [6], human albumin (HSA) [7], and liposomes [8]. The N-(2-hydroxypropyl)methacrylamide copolymer–DOX conjugate, additionally containing galactosamine (PK2), displayed effective liver-targeting ability [9] and diminished toxicity [10] in the earlier clinical studies. The enhanced antineoplastic efficacy in HCC was confirmed when DOX was conjugated to lactosaminated HSA [11] or encapsulated in galactose-conjugated liposomes [8]. In contrast, as the Gal-terminating drug conjugate is supposed to accumulate mainly in the liver because of large amounts of the ASGP-R present in hepatocytes [12,13], a problem arises, whether the Gal-terminating carriers tend to injure the remnant liver? This is a crucial point for effective HCC chemotherapy, but various responses have appeared. Some researchers have declared no detrimental effect in liver regeneration [14], and a healthy liver or a liver with fibrosis [15], some have described possible accompanying hepatic toxicity [9], whereas most researchers have ignored this problem. In addition, cardiotoxicity of the Gal-terminating drug conjugate is an aspect to be concerned

0959-4973 © 2011 Wolters Kluwer Health | Lippincott Williams & Wilkins DOI: 10.1097/CAD.0b013e3283406e85

about, as the cumulative dose-related cardiac damage is the limiting step in the use of DOX, as described everywhere [16,17].

With the aim to investigate the antitumor effect and hepatotoxicity of the liver-specific drug delivery system, we developed a Gal-terminated carrier for DOX based on our earlier study [18]. In that study, we had presented a new polymer-DOX conjugate by coupling DOX with α,β-poly[(2-hydroxyethyl)-L-aspartamide] (PHEA) with a succinic spacer. Such a PHEA–DOX conjugate displayed a higher therapeutic index and fewer adverse side effects than free DOX. In this study, we modified the PHEA–DOX conjugate with a Gal ligand to get the Gal–PHEA–DOX conjugate, and evaluated the therapeutic potential of this conjugate by assessing the in-vitro cell cytotoxicity, in-vivo distribution ability, in-vivo antitumor ability in both the subcutaneous sarcoma model and the orthotopic HCC model, and in-vivo systemic toxicity, especially hepatotoxcity and cardiotoxicity. These results suggested that the Gal–PHEA–DOX conjugate could bring enhanced antitumor efficacy with better tolerance *in vivo* for the treatment of HCC.

Materials and methods

Materials

L-aspartic acid, 1-ethyl-3-(3-dimethylaminopropyl)-carbodiimide, lactobionic acid (LA) and 3-(4,5-dimethylthiazd-2-yl)-2,5-diphenyltetrazolium bromide were purchased from Sigma Chemical Company (St Louis, Missouri, USA). DOX hydrochloride (purity > 98%) was purchased from Pharmacia & Upjohn Company (Milan, Italy). Enzymatic reagent kits for the determination of serum alanine aminotransferase (ALT), aspartate aminotransferase (AST), creatine kinase (CK), and lactate dehydrogenase (LDH) were purchased from Jiancheng Biochem. Ltd. (Nanjing, China). Methanol and acetonitrile were of chromatographic grade. Succinic anhydride, *n*-butanol, ethanolamine, N,N-dimethylformamide (DMF), 4-dimethylaminopyridine, sulfo-N-hydroxysuccinimide sodium salt, triethylamine, $AgNO_3$ and all other chemicals were of analytical grade and were used without further purification.

Animal models

Mouse sarcoma S180 cells were obtained from American Type Culture Collection. Mouse hepatoma solidity cells (Heps) expressing the ASGP-R were obtained from the Shanghai Institute of Cell Biology (Chinese Academy of Sciences, Shanghai, China). Both the cells were propagated by intraperitoneal (i.p.) implantation in female Institute of Cancer Research (ICR) mice. ICR mice (18–22 g) were obtained from the Experiment Animal Center of Nanjing Medical University (Nanjing, China), and maintained in plastic cages at 21 ± 2°C with free access to pellet food and water. All mice received humane care in accordance with the 'Guidelines for the Care and Use of Laboratory Animals' published by the National Institute of Health (NIH publication number 85-23, revised 1985).

Solid S180-bearing mice were prepared by inoculating 2.4×10^6 cells subcutaneously at the axillary region of the animals. The orthotopic model of HCC was established by direct intrahepatic injection of Heps cells according to the reported method [19] with modifications. In brief, the mice were anesthetized with 70 mg/kg sodium pentobarbital injected i.p. and then placed in a supine position on the procedure table. A small midline incision below the xyphoid was made to exteriorize the liver. Heps cells (1.0×10^7 cells/ml, 5 μl) were injected into the left hepatic lobe using a microinjector. After the injection, the pinprick was pressed with a sterile cotton swab to ensure hemostasis, and then sealed with NEXABAN Liquid topical tissue adhesive (Closure Medical Corporation, Raleigh, North Carolina, USA). The abdominal musculature and skin were closed with 6–0 silk sutures. The mice were kept in a warm cage until recovery from the anesthesia. Penicillin was given in drinking water to the mice for 3 days.

Preparation and characterization of the Gal–PHEA–DOX conjugate

PHEA and succinoylated PHEA (PHEA-suc) were synthesized and characterized as described earlier [18]. In brief, PHEA was synthesized by polymerization of L-aspartic acid with 85% phosphoric acid as a catalyst, followed by a ring-opening reaction with ethanolamine. PHEA-suc was prepared by esterifying the pendant hydroxyl groups of PHEA (0.5 g) with succinic anhydride (0.4 g), using 4-dimethylaminopyridine (30 mg) as a catalyst. The succinyl content of PHEA-suc was quantified by titration against a standard of NaOH (4×10^{-3} mol/l) using bromothymol blue as an indicator.

Gal–PHEA-suc was prepared by coupling the activated carboxyl group of LA with the hydroxyl group of PHEA-suc. A solution of N,N′,-carbonyldiimidazole (0.5 g) in 5 ml of anhydrous DMF was added dropwise at 0°C to a solution of LA (0.8 g) dissolved in 5 ml of dry DMF. The mixture was kept at 0°C for 1 h, followed by adding triethylamine (0.1 ml) and maintained at 0°C for 20 min. A solution of PHEA-suc (0.6 g) was added dropwise to this mixture, kept at 0°C for 15 min, then at 9°C for 1 h, and then finally set aside at room temperature for 3 days. Next, the solution was dialyzed against distilled water for 4 days and lyophilized. The degree of galactosylation was determined by the sulfuric acid micro-method [20].

DOX was conjugated to Gal–PHEA-suc using the reported method [18]. In brief, a solution of Gal–PHEA-suc (0.5 g) in 10 ml of DMF was mixed with 1-ethyl-3-(3-dimethylaminopropyl)-carbodiimide (0.5 g) and sulfo-N-hydroxysuccinimide

sodium salt (0.27 g) dissolved in 20 ml of DMF. The mixture was then added to DOX (125 mg) and triethylamine (60 μl), and gently stirred at room temperature for 24 h. The resulting conjugate was purified by gel-filtration using a Sephadex G25 column (Shanghai, China) with distilled water as the eluent and lyophilized. This process was kept away from light as much as possible.

The structure of Gal–PHEA–DOX was characterized by ^{1}H-NMR spectrometry (Bruker DRX-500, Switzerland). DOX content in the Gal–PHEA–DOX conjugate was measured by reverse-phase high-performance liquid chromatography (HPLC) with ultraviolet detection at 227 nm [21]. Briefly, free DOX encapsulated in the conjugate was extracted with isopropanol–chloroform (25 : 75, v/v) by mechanically shaking the samples for 30 min and then centrifugating the medium. The upper aqueous layer was removed by aspiration and the lower organic phase was transferred into a glass tube and evaporated to dryness. The residue was dissolved in the mobile phase for HPLC analysis. Total DOX in Gal–PHEA–DOX was determined after cleavage of the aminosugar moiety of DOX from the polymer conjugate. The Gal–PHEA–DOX solution was exposed to HCl (1.0 mol/l) at 85°C for 20 min, followed by the addition of phosphate buffer (0.5 mol/l, pH 7.4) and NaOH (1.0 mol/l), and then extracted and measured as that for free DOX.

HPLC analysis was performed using a Shimadzu HPLC system consisting of two pumps (LC-10Avp and LC-10AS) and a SPD-10Avp ultraviolet detector (Shimadzu Corporation, Japan). An Extend-C18 column (4.6 × 250 mm I.D., 5 μm) (Palo Alto, California, USA) was used. The mobile phase used for the analysis was a methanol–acetonitrile–phosphate buffer (pH 5.0; 0.2 mol/l) (50: 20: 30, v/v/v) and the flow rate was 0.5 ml/min.

Tissue distribution studies in tumor-bearing mice

In-vivo pharmacokinetics and biodistribution of Gal–PHEA–DOX were investigated in the Heps-bearing mice compared with those of DOX and PHEA–DOX. Nine days after the orthotopic injection of Heps cells, the mice were randomly divided into three groups, and intravenously (i.v.) injected with free DOX (10 mg/kg), PHEA–DOX [10 mg (DOX eq.)/kg], and Gal–PHEA–DOX [10 mg (DOX eq.)/kg], respectively. At various timepoints after the injection ($n = 5$ at each time point), whole blood was collected through cardiac puncture using a heparinized syringe, and plasma was prepared by centrifugation at 6000 rpm for 5 min. Several tissues, including the heart, liver, and tumor, were excised after killing the mice. Tissue samples were rinsed in PBS, blotted with paper towel, weighed, and homogenized in PBS.

In the PHEA–DOX-injected or Gal–PHEA–DOX-injected mice, both liberated DOX and total DOX content (including DOX in the conjugate form and DOX liberated from the conjugate) were quantified, respectively. Total DOX was determined after hydrolysis to generate aglycone and analyzed by HPLC as described above. Free DOX or liberated DOX was examined after protein denaturation [22,23]. In brief, tissue homogenate or plasma was added with $AgNO_3$ (3.0 mol/l), and the resulting suspension was mixed for 10 min at room temperature. The excess of silver ions was precipitated with NaCl (3.0 mol/l). Next, DOX was extracted and determined by HPLC as described earlier. Drug and Statistics for Windows (DAS ver 2.0; Beijing, China) was used to analyze the pharmacokinetic parameters of DOX for each formulation.

In-vitro cytotoxicity assay

Human cervix adenocarcinoma cells (HeLa) and HepG2 cells obtained from American Type Culture Collection were grown and maintained in RPMI-1640 medium, supplemented with 10% fetal bovine serum. The cells were seeded at a density of 1.0×10^4 cell/well in 96-well plates and allowed to grow for 24 h before treatment. The cells were treated with various concentrations of DOX and Gal–PHEA–DOX dissolved in saline for 24 h at 37°C. Cell number was measured using the 3-(4,5-dimethylthiazd-2-yl)-2,5-diphenyltetrazolium bromide cell viability assay.

In-vivo antitumor study

The antitumor activity of Gal–PHEA–DOX was examined in the subcutaneous S180-bearing mice after i.v. or intratumor (i.t.) administration and in the orthotopic Heps-bearing mice after i.v. administration at a dosage that was much higher than that administered weekly to humans (20 mg/m^2, corresponding to approximately 0.5 mg/kg).

S180-bearing mice were randomly assigned to four groups ($n = 10$). DOX, PHEA–DOX, and Gal–PHEA–DOX dissolved in saline were injected at a dose of 10 mg (DOX eq.)/kg on day 1 after tumor implantation. Saline was injected as a control. Another four groups ($n = 10$) of the S180-bearing mice were administrated with these formulations i.t. on day 8 at a dose of 5 mg (DOX eq.)/kg. Tumor size was measured from day 8 and tumor volume was calculated using the formula: $1/2 \times a \times b^2$, in which 'a' is the tumor dimension at the longest point, and 'b' is the width of the tumor. Mice body weight was recorded accordingly.

The therapeutic effect of Gal–PHEA–DOX was further investigated in the orthotopic model of HCC compared with DOX and PHEA–DOX. Heps-bearing mice were randomly assigned to four groups ($n = 6$) and injected i.v. through the tail vein with a total of 10 mg/kg of drugs dissolved in saline on days 1, 3, 5, and 7. Control mice received saline only. The mice were killed on day 12 and the tumors were excised and weighed. The tumor weight

of the treated group (T) was compared with that of the control group (C). The tumor inhibition rate was calculated as $(1–T/C) \times 100\%$.

Toxicological study

Histopathological study of the liver in Heps-bearing mice

For the Heps-bearing mice treated with saline, DOX, PHEA–DOX, or Gal–PHEA–DOX as mentioned in the antitumor study, liver samples were harvested on day 12 for histopathological study. Both the liver section adjacent to the tumor and the liver remnant in another hepatic lobe were investigated. The liver samples were immediately fixed in 10% buffered neutral formalin solution, transferred into gradient alcohol solutions, followed by embedding in paraffin, and sectioned at a thickness of 5 μm. Paraffin sections of the samples were stained with hematoxylin and eosin for microscopic observation. Histological analysis was carried out in a blind manner.

Safety assessment of Gal–PHEA–DOX in normal mice

The toxicity of Gal–PHEA–DOX in normal mice was investigated in the same batch as PHEA–DOX and DOX, which was presented in the earlier study [18]. Briefly, Gal–PHEA–DOX was i.p. injected into normal female ICR mice at doses of 6.0, 10.0, 16.7, 27.7, 46.3, and 77.3 mg (DOX eq.)/kg, respectively. Accordingly, the mice groups ($n = 10$) were designated as Gal–PHEA–DOX1 to Gal–PHEA–DOX6. Toxic symptoms and mortality were recorded thereafter for 14 days. At the end of 14 days, the mice that had survived were anesthetized with pentobarbital and recorded for electrocardiograms

Fig. 1

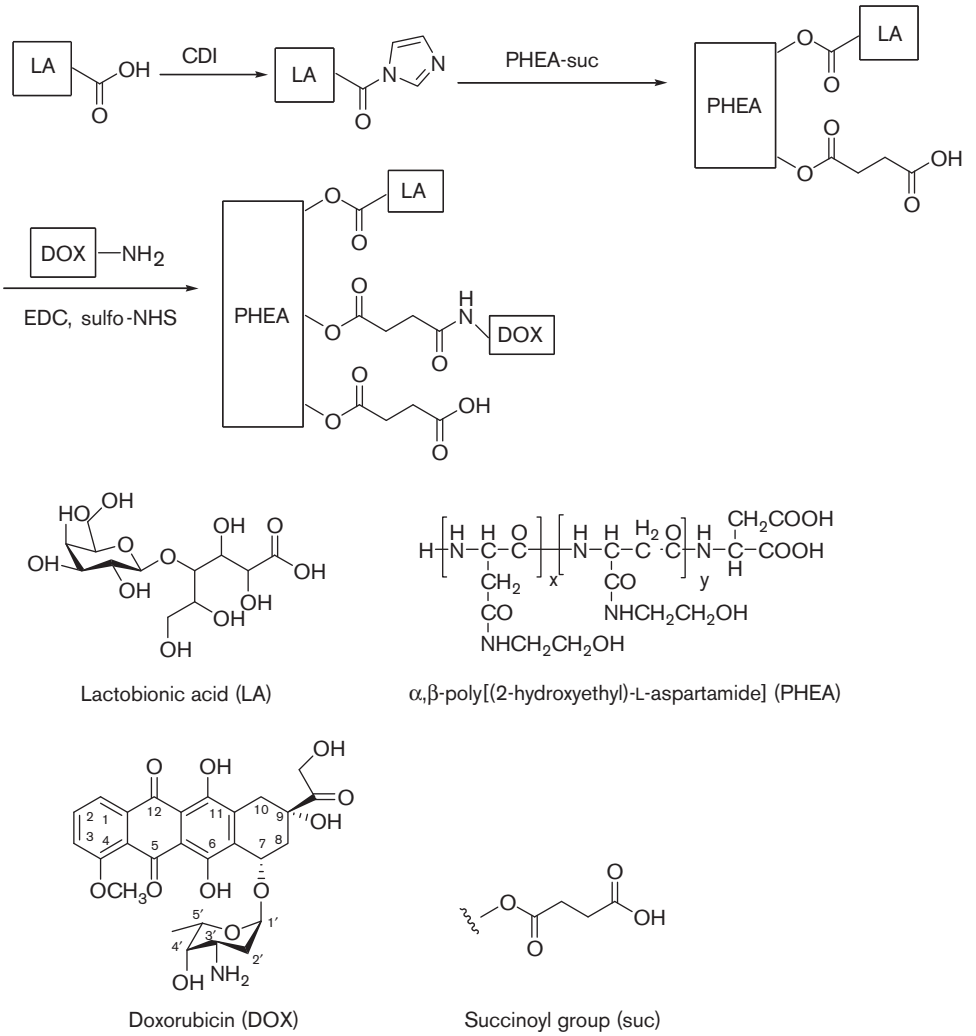

The synthesis route of galactosyl–α,β-poly[(2-hydroxyethyl)-L-aspartamide]–doxorubicin conjugate (Gal–PHEA–DOX). EDC, 1-ethyl-3-(3-dimethylaminopropyl)-carbodiimide; sulfo-NHS, sulfo-N-hydroxysuccinimide sodium salt.

(ECG) with the standard 12-lead synchronization high-frequency ECG system. Blood was collected though cardiac puncture and serum was tested for ALT, AST, CK, and LDH using enzymatic reagent kits.

Statistical analysis

Statistical analysis was performed using the Student's *t*-test for pairs of groups, and one-way analysis of variance for multiple groups. All results were expressed as the mean ± standard deviation unless otherwise noted. A probability (P) of less than 0.05 was considered statistically significant.

Results

Preparation and characterization of the Gal–PHEA–DOX conjugate

The synthesis of Gal–PHEA–DOX is outlined in Fig. 1. First, Gal–PHEA-suc was prepared by coupling the carboxyl group of LA with the hydroxyl residue of PHEA-suc. The formation of Gal–PHEA-suc was confirmed by the ^{1}H-NMR spectrum shown in Fig. 2a. The peaks at approximately 7.03, 4.24, and 4.12 ppm come from the LA residue [24]. The degree of succinoylation of PHEA-suc was detected to be 22.3 mol%. The substitution level of galactosylation in Gal–PHEA-suc was determined to be 7.5 mol%. Next, Gal–PHEA–DOX was obtained by linking the amino group of DOX with the carboxyl group of Gal–PHEA-suc. As shown in Fig. 2b, conjugation of DOX to the polymer is confirmed by the presence of characteristic peaks of DOX at 5.56, 5.22, 3.99, and 1.23 ppm [25]. DOX content in Gal–PHEA–DOX was determined to be 8.9 wt% using HPLC, with no remarkable amount of free DOX (less than 2 wt% of the total DOX content) after purification.

Fig. 2

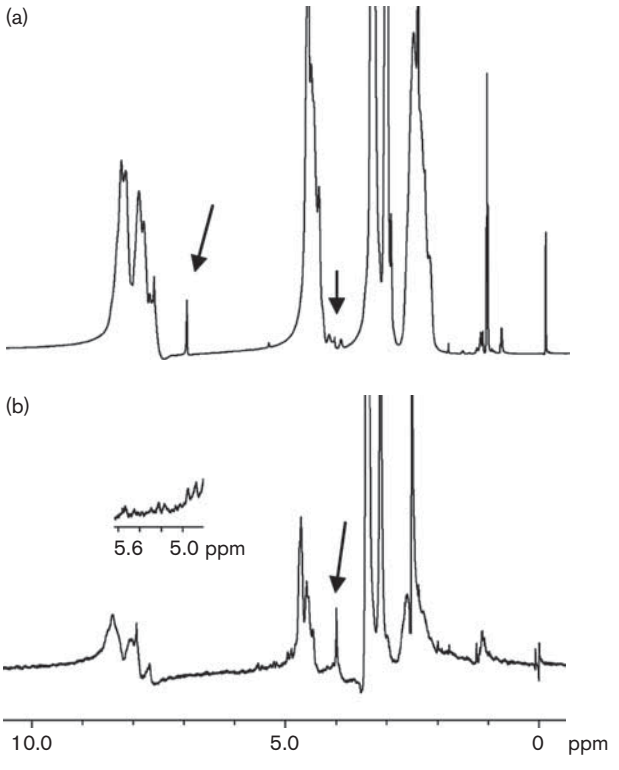

^{1}H-NMR spectra of galactosyl–succinoylated α,β-poly[(2-hydroxyethyl)-L-aspartamide] and galactosyl–α,β-poly[(2-hydroxyethyl)-L-aspartamide]–doxorubicin conjugate in dimethyl sulfoxide-d6.

In-vivo pharmacokinetic studies

To estimate the potential increase in the chemotherapeutic index and decrease in the side effects of Gal–PHEA–DOX, the drug level of Gal–PHEA–DOX in the Heps-bearing mice was measured in the plasma, tumor, liver, and heart as compared with that of free DOX or PHEA–DOX. In the PHEA–DOX-injected or Gal–PHEA–DOX-injected mice, the drug forms determined in the plasma or organs were both DOX in the conjugate form and DOX liberated from the conjugate. The concentration–time profiles of total DOX and free/liberated DOX in the plasma, liver, heart, or tumor are shown in Fig. 3a–h, respectively.

In plasma, Gal–PHEA–DOX administration produced a slightly lower concentration of total DOX than that of PHEA–DOX, but much higher than that of free DOX that was cleared from the bloodstream rapidly (Fig. 3a). The values of the area under the plasma concentration–time curve ($AUC_{0-\infty}$) for Gal–PHEA–DOX were seven times higher than that of free DOX (Table 1). On account of the polymer conjugate circulated at a high concentration for an extended period, DOX liberated from both the conjugates retained a high level compared with free DOX (Fig. 3e).

In accordance with the sustained residence in blood, the longer circulating conjugates were more efficiently accumulated in the liver, heart, or tumor than the free DOX formulation. As expected, the liver uptake of Gal–PHEA–DOX was much higher than that of the nongalactosylated PHEA–DOX and free DOX (Fig. 3b). Although the liver contained a substantial amount of Gal–PHEA–DOX, there was a marked decrease of liberated DOX from this conjugate as compared with the distribution of DOX in case of free DOX administration (Fig. 3f). PHEA–DOX liberated a similar drug level as that of Gal–PHEA–DOX. When administered with Gal–PHEA–DOX, the free drug concentration peak (C_{max}) was four times lower than that of DOX administration (Table 2).

Both Gal–PHEA–DOX and PHEA–DOX displayed similar distribution trends in the heart, not only for the polymer-bound total DOX but also for the free DOX liberated from these conjugates (Fig. 3c and g). The AUC and C_{max} of the liberated DOX from Gal–PHEA–DOX decreased three and four times than that of the DOX formulation, respectively (Table 2).

Fig. 3

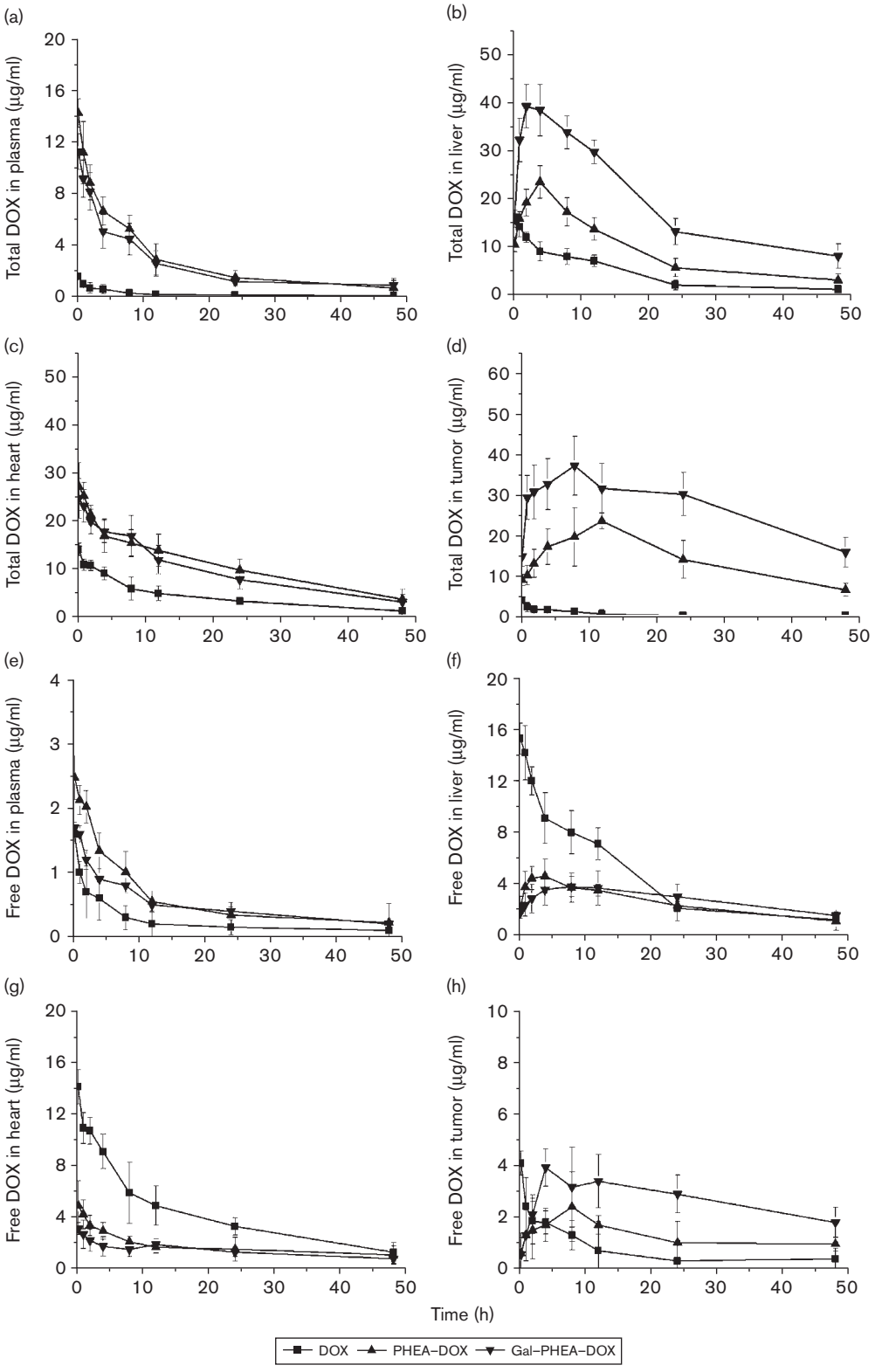

Comparison of the body distribution of galactosyl–α,β-poly[(2-hydroxyethyl)-L-aspartamide]–doxorubicin conjugate (Gal–PHEA–DOX) with DOX and PHEA–DOX administered intravenously [10 (DOX eq.) mg/kg] in the Heps-bearing mice. Total doxorubicin levels in the (a) plasma; (b) liver; (c) heart; (d) tumor; and free or liberated doxorubicin in the (e) plasma; (f) liver; (g) heart; (h) tumor. Results are expressed as the mean ± SE ($n = 5$).

Tumor levels of total DOX followed a similar pattern to those observed in the liver (Fig. 3d and h). Gal–PHEA–DOX accumulated at the highest level in the tumor. The tumor AUC of total drug of Gal–PHEA–DOX increased by nearly 2-fold and 40-fold as compared with PHEA–DOX and DOX formulation, respectively. In addition, Gal–PHEA–DOX produced a four-fold larger AUC of liberated DOX in the tumor than free DOX.

In-vitro cytotoxicity assay

To investigate the activity and HCC-targeting ability of Gal–PHEA–DOX, HeLa and human HCC cells (HepG2) expressing ASGP-R were used for the cytotoxicity assay. Figure 4 shows the results of cell viability treated with Gal–PHEA–DOX. The cytotoxicity of free DOX was not presented as the IC_{50} values of DOX (2.72 μg/ml in HeLa cells and 4.22 μg/ml in HepG2 cells) were similar to those in the earlier study [18]. Gal–PHEA–DOX displayed less sensitivity than free DOX in both the cells. The IC_{50} values of the Gal–PHEA–DOX at 24 h were calculated to be 47.01 μg (DOX eq.)/ml in HeLa cells and 18.03 μg (DOX eq.)/ml in HepG2 cells, respectively. Although Gal–PHEA–DOX was less effective in HeLa cells than PHEA–DOX [29.80 μg (DOX eq.)/ml], it displayed a superior inhibition activity in HepG2 cells as compared with the nontargeted PHEA–DOX conjugate [45.93 (DOX eq.) μg/ml] [18].

In-vivo antitumor study

The therapeutic effect of Gal–PHEA–DOX was compared with PHEA–DOX and DOX in both the subcutaneous sarcoma S180 model and the orthotopic hepatic Heps tumor model as shown in Fig. 5.

The antitumor activity of Gal–PHEA–DOX in the S180 model was evaluated through two administration routes. When given i.v. on day 1 after tumor implantation, Gal–PHEA–DOX could inhibit tumor growth, but was not as efficient as DOX. Neither was the PHEA–DOX conjugate

Table 1 Plasma pharmacokinetic parameters of the Gal–PHEA–DOX conjugate compared with those of PHEA–DOX or DOX after intravenous injection in the Heps-bearing mice at a single equivalent dose of 10 mg/kg

		PHEA–DOX		Gal–PHEA–DOX	
	DOX	Total DOX	Liberated DOX	Total DOX	Liberated DOX
$t_{1/2\alpha}$ (h)	0.355	0.697	4.014	1.579	1.974
$t_{1/2\beta}$ (h)	5.881	8.615	57.059	12.544	31.816
$MRT_{0-\infty}$ (h)	12.968	17.552	23.391	15.476	40.034
$AUC_{0-\infty}$ (μg h/ml)	10.783	146.442	28.64	138.25	39.156
CLz (l/h/kg)	1.855	0.137	0.698	0.145	0.511
Vdz (l/kg)	25.478	2.685	10.206	3.654	20.616

$AUC_{0-\infty}$, area under the plasma concentration–time curves; CLz, total body clearance; Gal–PHEA–DOX, galactosyl–α,β-poly[(2-hydroxyethyl)-L-aspartamide]–doxorubicin conjugate; $MRT_{0-\infty}$, mean residence time; $t_{1/2\alpha}$, distribution half-life; $t_{1/2\beta}$, elimination half-life; Vdz, volume of distribution.

Fig. 4

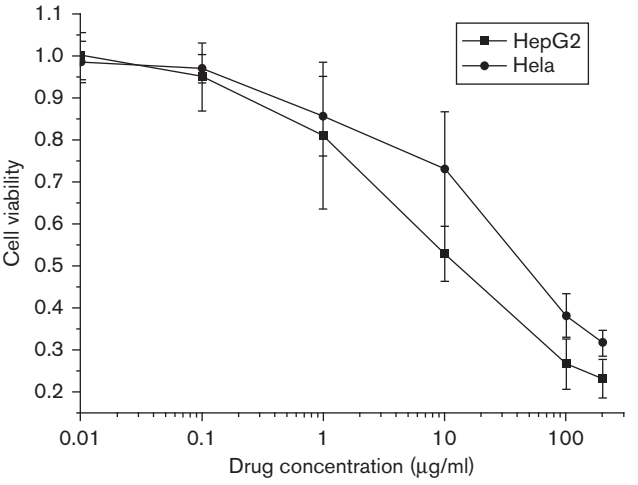

In-vitro cytotoxicity evaluation of galactosyl–α,β-poly[(2-hydroxyethyl)-L-aspartamide]–doxorubicin conjugate in human cervix adenocarcinoma cells (HeLa) cells and HepG2 cells after incubation for 24 h.

Table 2 Tissue pharmacokinetic parameters of the Gal–PHEA–DOX conjugate compared with those of PHEA–DOX or DOX after intravenous injection in the Heps-bearing mice at a single equivalent dose of 10 mg/kg

		PHEA–DOX		Gal–PHEA–DOX	
	DOX	Total DOX	Liberated DOX	Total DOX	Liberated DOX
Liver					
$AUC_{0.25-48\,h}$ (μg h/g)	208.487	438.883	124.398	921.444	134.727
T_{max} (h)	0.25	4.0	2.0	4.0	8.0
C_{max} (μg/g)	15.31	23.55	4.65	39.21	3.78
Heart					
$AUC_{0.25-48\,h}$ (μg h/g)	200.846	517.931	82.852	460.835	64.739
T_{max} (h)	0.25	0.25	0.25	0.25	0.25
C_{max} (μg/g)	14.01	27.12	4.91	24.77	3.12
Tumor					
$AUC_{0.25-48\,h}$ (μg h/g)	34.365	692.262	62.371	1323.079	131.075
T_{max} (h)	0.25	12.0	8.0	8.0	4.0
C_{max} (μg/g)	4.13	23.77	2.45	37.36	3.93

$AUC_{0.25-48\,h}$, area under the tissue DOX concentration–time curves; C_{max}, maximum concentration; Gal–PHEA–DOX, galactosyl–α,β-poly[(2-hydroxyethyl)-L-aspartamide]–doxorubicin conjugate; T_{max}, corresponding time.

Fig. 5

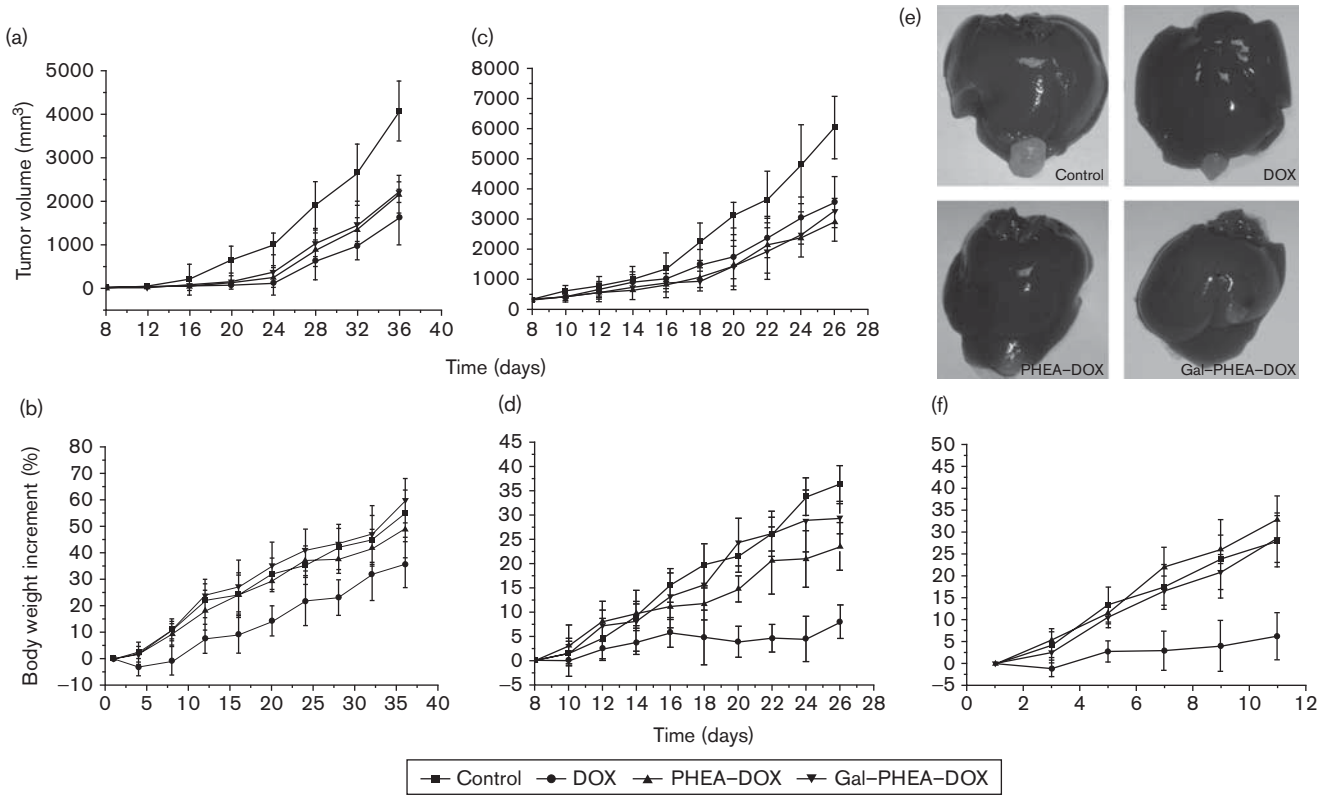

Therapeutic effects of galactosyl–α,β-poly[(2-hydroxyethyl)-L-aspartamide]–doxorubicin conjugate (Gal–PHEA–DOX) compared with DOX and PHEA–DOX in the subcutaneous S180-bearing mice after a single intravenous injection (10 mg/kg): (a) tumor inhibition effect and (b) changes in mice body weight; in the subcutaneous S180-bearing mice after a single intratumoral injection (5 mg/kg), (c) tumor inhibition effect, and (d) changes in mice body weight; and in orthotopic Heps-bearing mice after multiple intravenous doses (total 10 mg/kg), (e) typical photographs of the liver bearing Heps tumor and (f) changes in mice body weight.

Table 3 In-vivo antitumor study of Gal–PHEA–DOX compared with DOX and PHEA–DOX in orthotopic Heps-bearing mice after multiple intravenous doses (total 10 mg/kg)

Drug	Saline control	DOX	PHEA–DOX	Gal–PHEA–DOX
Tumor inhibition rate (%)	–	48.3%	55.7%	79.1%*

Gal–PHEA–DOX, galactosyl–α,β-poly[(2-hydroxyethyl)-L-aspartamide]–doxorubicin conjugate.
*Significantly different from control ($P<0.05$).

(Fig. 5a). Figure 5c shows that Gal–PHEA–DOX displays a similar tumor inhibition rate as PHEA–DOX and exhibits more antitumor efficacy than free DOX when injected i.t. on day 8. For the Heps tumor model, Gal–PHEA–DOX markedly inhibited tumor growth, whereas both DOX and PHEA–DOX displayed moderate antitumor efficacy after multiple i.v. doses (2.5 mg/kg × 4 times) (Fig. 5e). Gal–PHEA–DOX, PHEA–DOX, and DOX induced tumor volume reductions of 79.1 ($P<0.05$), 55.7, and 48.3% (Table 3), respectively, compared with the saline-treated group.

Among all the experimental models, body weight loss or low weight increment was only observed in the DOX-treated groups. Growth in the mice did not seem to be significantly influenced by treatments of either Gal–PHEA–DOX or PHEA–DOX, indicating a much-relieved toxicity in mice as shown in Fig. 5b, d and f.

Toxicological study

Histopathological studies of liver sections were carried out to examine whether Gal–PHEA–DOX impaired the liver when it enhanced the antitumor effect in HCC. The microscopic structures of both the liver section adjacent to the tumor in the left lobe and the liver remnant in the right lobe in the Heps-bearing mice are shown in Fig. 6. No histologic lesions were found in the liver of the control mice. The liver sections of the mice treated with DOX showed parenchymal degeneration, and apoptotic and necrotic hepatocytes. These effects appeared mildly in the liver of the mice treated with PHEA–DOX. Although the Gal–PHEA–DOX conjugate selectively accumulated in the liver, it caused negligible detrimental

Fig. 6

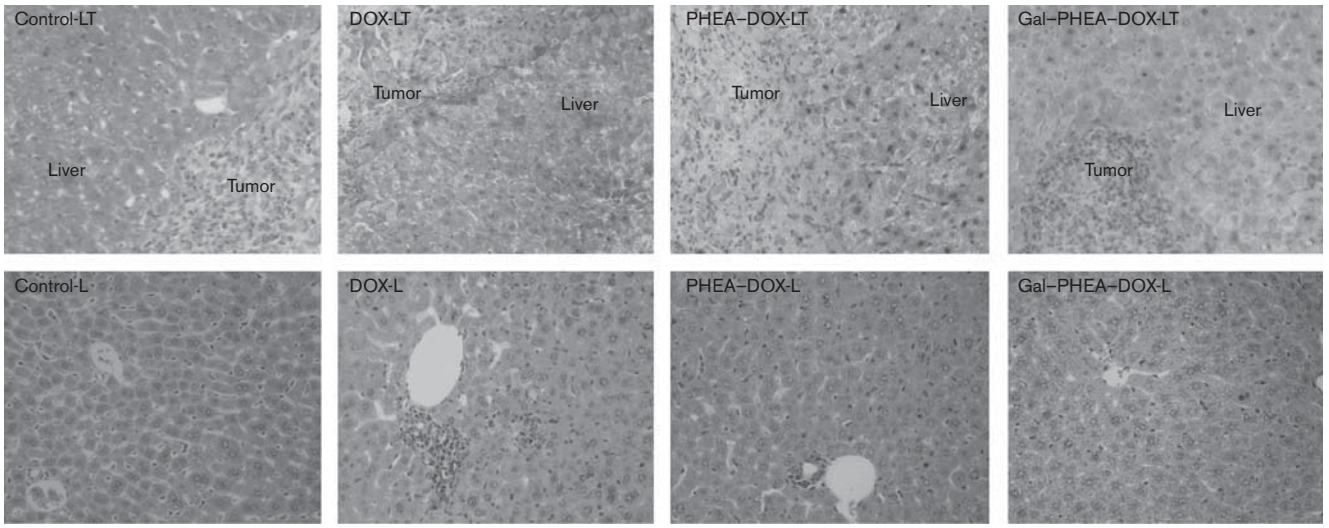

Photomicrographs of the liver (L) section adjacent to the tumor (T) [control-LT, doxorubicin (DOX)-LT, –α,β-poly[(2-hydroxyethyl)-L-aspartamide] (PHEA)–DOX-LT, and galactosyl (Gal)–PHEA–DOX-LT) and the liver remnant in another lobe (control-L, DOX-L, PHEA–DOX-L and Gal–PHEA–DOX-L) in the Heps-bearing mice at day 12 after treatments with saline, DOX, PHEA–DOX, and Gal–PHEA–DOX, respectively.

effect on the histology of the liver, which indicated that Gal–PHEA–DOX would not damage the liver remnant when it was used in HCC chemotherapy.

The side effects (especially cytotoxicity and hepatotoxicity) of Gal–PHEA–DOX were further investigated in normal mice in the same batch as DOX and PHEA–DOX, as reported [18]. The Gal–PHEA–DOX-treated groups were associated with more alleviated piloerection, adynamia, hypodynamia than the DOX-treated groups.

Administration of Gal–PHEA–DOX caused no mortality at all the doses, indicating that the median lethal dose (LD_{50}) was greater than 77.3 mg (DOX eq.)/kg. The safety effect of Gal–PHEA–DOX was much improved as compared with DOX (LD_{50} of DOX: 19.63 mg/kg [18]).

Two weeks after the treatment with Gal–PHEA–DOX, the analysis of the ECG tracing was carried out by measuring the duration and voltage of the QRS complex.

As shown in Fig. 7a, the Gal–PHEA–DOX-treated mice showed mild changes in ECG at the dose of 22.7 mg (DOX eq.)/kg (Gal–PHEA–DOX4 group), which is similar to that of the PHEA–DOX4 group, but much alleviated as compared with the DOX4 group. Gal–PHEA–DOX caused a pronounced tachycardia only at the highest dosage of 77.3 mg (DOX eq.)/kg. The significant prolongation of the P–R interval was observed only in the mice that had received a dosage higher than 46.3 mg (DOX eq.)/kg, whereas no significant change in the Q–T interval was observed in all the Gal–PHEA–DOX-treated groups (Fig. 7b and c). This indicated the reduced cardiotoxicity of DOX given in the form of Gal–PHEA–DOX. The alleviative effect of Gal–PHEA–DOX on the heart was further supported by the fact that no significant increase in the level of the CK or LDH enzyme occurred below the dosage of 27.7 mg (DOX eq.)/kg (Table 4).

Hepatotoxicity of Gal–PHEA–DOX was evaluated using the serum biochemical parameters and relative liver weight reported in Table 4. The Gal–PHEA–DOX conjugate did not produce significant change in AST, ALT, LDH, and liver weight when the dosage used was not higher than 27.7 mg (DOX eq.)/kg. In another way, the free DOX formulation tended to change the serum biochemical parameters at every tested dosage, as reported [18]. The toxicity study indicated that the Gal–PHEA–DOX conjugate was well tolerated even at a dose three times higher than that of free DOX.

Discussion

The ASGP-R is known to be an excellent target for receptor-mediated liver-specific drug delivery. As it has a high affinity for clusters of galactose residues, various Gal-terminating carriers have been developed for restricting drug action in the liver. Improved chemotherapy for HCC is achieved by such Gal-terminated drug delivery systems because of the presence of ASGP-R in the cell plasma membrane in all the cells of the majority of well-differentiated HCCs, including the proliferating ones [5]. However, as ASGP-R is expressed at a higher density in normal hepatocytes than in HCC cells [26], the Gal-terminated drug delivery system may run the risk of causing detrimental effects on the healthy liver. This study aimed at developing a galactosylated polymer conjugate of DOX (Gal–PHEA–DOX), and evaluating

Fig. 7

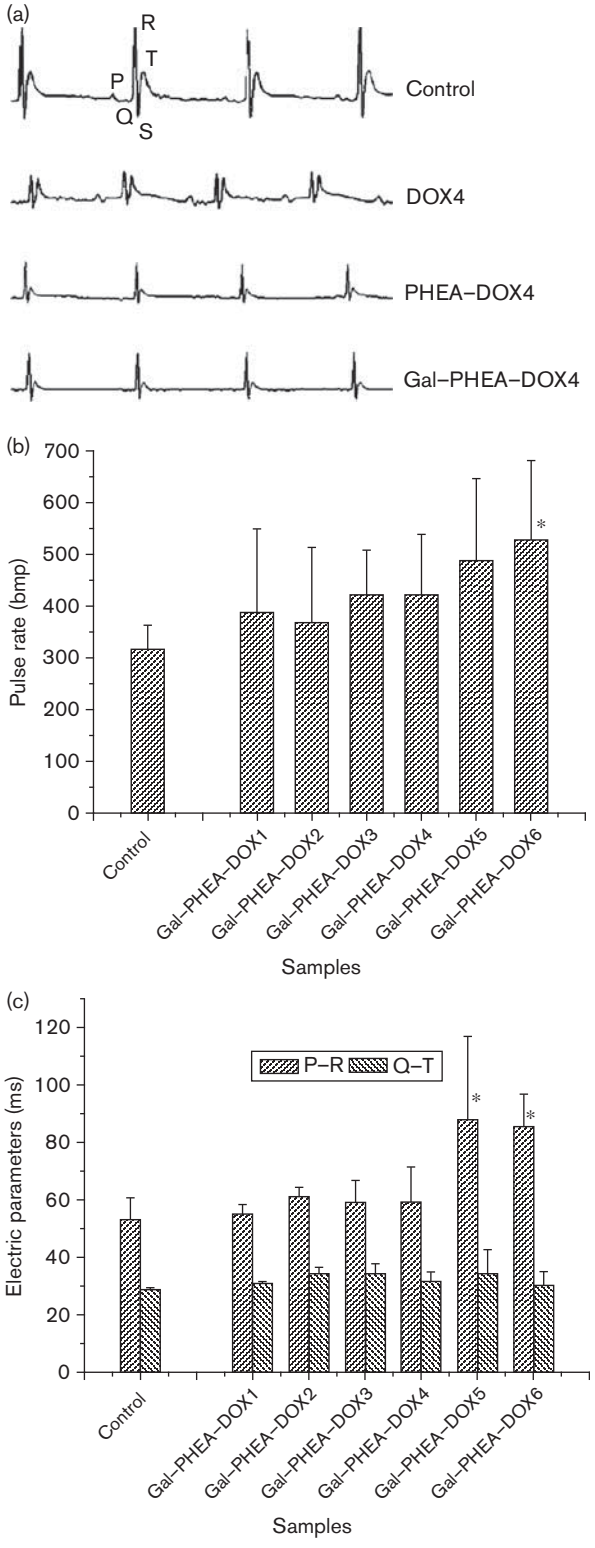

Electrocardiograph (a), pulse rate (b), and P–R-interval or Q–T-interval of mice (c) at day 14 after administration of galactosyl–α,β-poly[(2-hydroxyethyl)-L-aspartamide]–doxorubicin conjugate (Gal–PHEA–DOX). *Significantly different from control ($P<0.05$).

its antitumor efficacy in HCC and the possible associated side effects, especially hepatotoxicity and cardiotoxicity. The rationale for the development of a Gal–PHEA–DOX conjugate was to improve hepatic tumor targeting. The promising biological activity of the Gal–PHEA–DOX conjugate can be shown by comparison with that of the nontargeted conjugate PHEA–DOX and that of free DOX.

Gal–PHEA–DOX was prepared by sequentially coupling LA and DOX with the precursor polymer of PHEA-suc as reported in our earlier study [18]. The therapeutic effects of the Gal–PHEA–DOX conjugate were analyzed considering its in-vivo pharmacokinetics.

Before the in-vivo therapeutic evaluation, potential antitumor activity and hepatotropic ability of the Gal–PHEA–DOX conjugate were verified in both the HeLa and HepG2 cells. Gal–PHEA–DOX displayed lower cytotoxicity than DOX in both the cell lines because of the changed cellular pharmacokinetics such as slower endocytosis compared with the rapid transmembrane passage of the free drug [27,28]. Gal–PHEA–DOX showed higher cell inhibition ability than PHEA–DOX in HepG2 cells despite the fact that it was not as active as PHEA–DOX in HeLa cells, indicating that the Gal–PHEA–DOX conjugate could be selectively taken up by HCC cells.

Gal-terminated drug delivery systems were usually evaluated in the subcutaneous tumor models [29] or diethylnitrosamine-induced HCCs [11]. The former model could not absolutely reflect the therapeutic efficacy in primary liver tumors, whereas the latter model was time exhausted. This study established an orthotopic hepatocarcinoma model by directly injecting Heps cells into the liver, which could easily obtain high efficiency and form a primary tumor in a microenvironment close to the one it originated from [19]. The Gal–PHEA–DOX conjugate achieved better antitumor efficacy than free DOX or the nongalactosylated PHEA–DOX conjugate in the orthotopic Heps-bearing mice, which could be attributed to the enhanced accumulation of Gal–PHEA–DOX in HCCs and a sustained release of the free drug from this conjugate. Both the passive and active targeting strategies contributed to the accumulation of Gal–PHEA–DOX in the hepatoma, which could be elucidated by its therapeutic effects in the different tumor models or the pharmacokinetics index. First, the Gal–PHEA–DOX conjugate could passively accumulate in the tumor. As investigated in the S180 models, the antitumor efficacy of Gal–PHEA–DOX varied with the different administration regimens as compared with free DOX, but was not significantly different from that of PHEA–DOX. The Gal–PHEA–DOX conjugate displayed less inhibition activity in the S180 tumor than DOX when administered on day 1 (Fig. 5a), but was more efficient as compared

Table 4 Serum biochemical parameters and relative liver weight at day 14 after the administration of different doses of Gal–PHEA–DOX to mice

	Dose [mg (DOX eq.)/kg]	ALT (U/l)	AST (U/l)	AST/ALT	LDH (U/l)	CK (U/ml)	Liver weight/body weight (%)
Control	–	27.3 ± 2.3	31.5 ± 2.6	1.15	474.4 ± 74.3	0.22 ± 0.18	6.44 ± 0.41
Gal–PHEA–DOX1	6.0	26.0 ± 4.9	32.5 ± 4.5	1.25	486.1 ± 35.3	0.19 ± 0.03	6.24 ± 0.86
Gal–PHEA–DOX2	10.0	28.1 ± 3.0	34.1 ± 7.4	1.21	470.1 ± 61.7	0.30 ± 0.37	6.12 ± 0.42
Gal–PHEA–DOX3	16.7	27.1 ± 3.1	31.3 ± 2.6	1.15	474.9 ± 54.3	0.38 ± 0.11	6.55 ± 0.35
Gal–PHEA–DOX4	27.7	25.2 ± 5.8	34.4 ± 5.2	1.36	517.8 ± 68.8	0.58 ± 0.23*	6.27 ± 0.02
Gal–PHEA–DOX5	46.3	25.9 ± 4.2	36.3 ± 5.1*	1.40	541.9 ± 63.1*	0.87 ± 0.45*	7.26 ± 0.41*
Gal–PHEA–DOX6	77.3	24.3 ± 3.1*	38.4 ± 4.8*	1.58	557.4 ± 52.3*	1.15 ± 0.48**	7.13 ± 0.60*

ALT, alanine aminotransferase; AST, aspartate aminotransferase; CK, creatine kinase; Gal–PHEA–DOX, galactosyl–α,β-poly[(2-hydroxyethyl)-L-aspartamide]–doxorubicin conjugate; LDH, lactate dehydrogenase.
*Significantly different from control ($P<0.05$).
**Significantly different from control ($P<0.001$).

with DOX when administered to the mice on day 8 (Fig. 5c) after tumor implantation. This is because in the latter case the tumor was palpable and provided specific structural conditions to entrap the conjugates, which is indicated as 'the enhanced permeability and retention effect'. As the S180 tumor lacked specific selectivity for the galactose moiety, Gal–PHEA–DOX was endocytosed similarly to PHEA–DOX and showed comparable therapeutic effects to that of PHEA–DOX. Second, the Gal–PHEA–DOX conjugate was further taken up into the HCC cell by ASGP-R recognition. It was reported that a lactosaminated HSA conjugate of DOX enhanced drug accumulation in all the forms of rat HCCs, including those which do not express the ASGP-R [30]. The superior therapeutic ability of Gal–PHEA–DOX to PHEA–DOX in the Heps-bearing mice came from the actively accumulated drugs. Furthermore, the accumulation of Gal–PHEA–DOX in the tumor was verified by the pharmacokinetic index (Fig. 3d). A higher dose intensity of Gal–PHEA–DOX than PHEA–DOX in Heps tumor suggested selective recognition by the galactose ligand, whereas PHEA–DOX accumulated more than DOX because of the enhanced permeability and retention effect. However, the carboamide bond linking DOX to the carrier PHEA resulted in slowly-cleaved active drugs. The release characteristics may be improved by using an easily hydrolyzed bond, such as the hydrazone bond, which can facilitate site-specific drug release in the tumor [31].

As Gal–PHEA–DOX is hepatotropic because of ASGP-R recognition, one might speculate that the targeted delivery of DOX to the liver may be associated with hepatic dysfunction. We investigated the liver histology in the Heps-bearing mice and found that the Gal–PHEA–DOX conjugate did not cause any risks to the liver remnant when it efficiently inhibited heptocarcinoma growth contemporarily. It is believed [32] that the release of DOX from its polymeric carrier is a prerequisite for the pharmacological activity of the conjugate. Thus, toxicity could be predicted by the liberated DOX exposure in tissues, such as AUC, C_{max}, and distribution variables [33]. Although Gal–PHEA–DOX is highly accumulated in the liver, free DOX liberated from this conjugate is not damaging. Both AUC and C_{max} of liberated DOX from the Gal–PHEA–DOX conjugate were much lower than those of DOX administration (Fig. 3b), indicating relieved side effects of this conjugate.

We were encouraged by the much-relieved hepatotoxcity of Gal–PHEA–DOX in the HCC model, and thus explored the systemic side effects of this conjugate in normal mice. On account of the sustained release of DOX from the conjugate and the relatively low concentration peak in various tissues, a longer survival time in mice and reduced cardiotoxicity and hepatotoxity were achieved when DOX was administered in the Gal–PHEA–DOX conjugate form. This indicates that the Gal–PHEA–DOX conjugate can be administered at a greater elevating dose in chemotherapy as compared with free DOX. In fact, our earlier study [18] has shown that an increased PHEA–DOX dosage was associated with enhanced antitumor efficacy.

Taken together, these studies showed that Gal–PHEA-DOX had better therapeutic effects than free DOX in HCC, and also significantly reduced hepatotoxicity and other side effects associated with DOX.

Conclusion

A liver-targeting Gal–PHEA–DOX conjugate was developed in this study. This conjugate achieved greater drug levels in hepatic tumors than the nongalactosylated PHEA–DOX conjugate or free DOX, thus providing satisfactory therapeutic effects in the orthotopic murine model bearing hepatoma. Despite high accumulation in the liver, Gal–PHEA–DOX showed relieved liver side effects in the HCC model, which could be attributed to the low free DOX content liberated from the conjugate. The Gal–PHEA–DOX conjugate also showed better tolerance in normal mice than free DOX with regard to cytotoxicity and hepatotoxicity. These results indicate that the Gal–PHEA–DOX conjugate has the potential for use in HCC chemotherapy.

Acknowledgements

This study was supported by the National Natural Science Foundation of China (nos. 50673041 and

30771036), the National Basic Research Foundation of China (973 Programs 2006CB503908 and 2004CB51 8603), the Chinese National Programs for High Technology Research and Development (863 Program 2006AA 02Z177), National Pharmaceutical Program (2009ZX095 03-028), and the 111 project from the Chinese Ministry of Education.

References

1 Olweny CL, Toya T, Katongole-Mbidde E, Mugerwa J, Kyalwazi SK, Cohen H. Treatment of hepatocellular carcinoma with adriamycin. *Cancer* 1975; **36**:1250–1257.
2 Leung TWT, Johnson PJ. Systemic therapy for hepatocellular carcinoma. *Semin Oncol* 2001; **28**:514–520.
3 Huang CC, Wu MC, Xu GW, Li DZ, Cheng H, Tu ZX, *et al.* Overexpression of the MDR1 gene and P-glycoprotein in human hepatocellular carcinoma. *J Natl Cancer Inst* 1992; **84**:262–264.
4 Nowak AK, Chow PK, Findlay M. Systemic therapy for advanced hepatocellular carcinoma: a review. *Eur J Cancer* 2004; **40**:1474–1484.
5 Trerè D, Fiume L, De Giorgi LB, Di Stefano G, Migaldi M, Derenzini M. The asialoglycoprotein receptor in human hepatocellular carcinomas: its expression on proliferating cells. *Br J Cancer* 1999; **81**:404–408.
6 Duncan R. Designing polymer conjugates as lysosomotropic nanomedicines. *Biochem Soc Trans* 2007; **35**:56–60.
7 Di Stefano G, Lanza M, Kratz F, Merina L, Fiume L. A novel method for coupling doxorubicin to lactosaminated human albumin by an acid sensitive hydrazone bond: synthesis, characterization and preliminary biological properties of the conjugate. *Eur J Pharm Sci* 2004; **23**:393–397.
8 Matsuda I, Konno H, Tanaka T, Nakamura S. Antimetastatic effect of hepatotropic liposomal adriamycin on human metastatic liver tumors. *Surg Today* 2001; **31**:414–420.
9 Seymour LW, Ferry DR, Anderson D, Hesslewood S, Julyan PJ, Poyner R, *et al.* Hepatic drug targeting: phase I evaluation of polymer-bound doxorubicin. *J Clin Oncol* 2002; **20**:1668–1676.
10 Hopewell JW, Duncan R, Wilding D, Chakrabarti K. Preclinical evaluation of the cardiotoxicity of PK2: a novel HPMA copolymer–doxorubicin–galactosamine conjugate antitumour agent. *Hum Exp Toxicol* 2001; **20**:461–470.
11 Fiume L, Bolondi L, Busi C, Chieco P, Kratz F, Lanza M, *et al.* Doxorubicin coupled to lactosaminated albumin inhibits the growth of hepatocellular carcinomas induced in rats by diethylnitrosamine. *J Hepatol* 2005; **43**:645–652.
12 O'Hare KB, Hume IC, Carlett SL, Duncan R. Evaluation of anticancer agents coupled to N-(2-hydroxypropyl)-methacrylamide copolymers. Effect of galactose incorporation on interaction with hepatoma *in vitro*. *Hepatology* 1989; **10**:207–214.
13 Seymour LW, Ulbrich K, Strohalm J, Duncan R. Pharmacokinetics of a polymeric drug carrier targeted to the hepatocyte galactose receptor. *Br J Cancer* 1991; **63**:859–866.
14 Di Stefano G, Derenzini M, Kratz F, Lanza M, Fiume L. Liver-targeted doxorubicin: effects on rat regenerating hepatocytes. *Liver Int* 2004; **24**:246–252.
15 Xu ZH, Chen LL, Gu WW, Gao Y, Lin LP, Zhang ZW, *et al.* The performance of docetaxel-loaded solid lipid nanoparticles targeted to hepatocellular carcinoma. *Biomaterials* 2009; **30**:226–232.
16 Injac R, Perse M, Cerne M, Potocnik N, Radic N, Govedarica B, *et al.* Protective effects of fullerenol $C_{60}(OH)_{24}$ against doxorubicin-induced cardiotoxicity and hepatotoxicity in rats with colorectal cancer. *Biomaterials* 2009; **30**:1184–1196.
17 Raschi E, Vasina V, Ursino MG, Boriani G, Martoni A, De Ponti F. Anticancer drugs and cardiotoxicity: insights and perspectives in the era of targeted therapy. *Pharmacol Ther* 2010; **125**:196–218.
18 Cheng XY, Xue WH, Diao HJ, Xia SH, Zuo LS, He AJ, *et al.* Antitumor activity and toxicological properties of doxorubicin conjugated to α,β-poly[(2-hydroxyethyl)-L-aspartamide] administrated intraperitoneally in mice. *Anticancer Drugs* 2010; **21**:362–371.
19 Pavlaki M, Zucker S. Matrix metalloproteinase inhibitors (MMPIs): the beginning of phase I or the termination of phase III clinical trials. *Cancer Metastasis Rev* 2003; **22**:177–203.
20 Monsigny M, Petit C, Roche AC. Colorimetric determination of neutral sugars by a resorcinol sulfuric acid micromethod. *Anal Biochem* 1988; **175**:525–530.
21 Frauer D, Frigerio E, Pianezzola E, Strolin Benedetti M, Cassidy J, Vasey P. A sensitive procedure for the quantitation of free and N-(2-hydroxypropyl) methacylamide polymer-bound doxorubicin (PK1) and some of its metabolites, 13-dihydrodoxorubicin, 13-dihydrodoxorubicinone and doxorubicinone, in human plasma and urine by reversed-phase HPLC with fluorimetric detection. *J Pharm Biomed Anal* 1995; **13**:625–633.
22 Seymour LW, Ulbrich K, Strohalm J, Kopecek H, Duncan R. The pharmacokinetics of polymer-bound adriamycin. *Biochem Pharmacol* 1990; **39**:1125–1131.
23 Mürdtera TE, Sperkera B, Bossletb K, Fritza P, Kroemer HK. Simultaneous high-performance liquid chromatographic determination of a glucuronyl prodrug of doxorubicin, doxorubicin and its metabolites in human lung tissue. *J Chromatogr B* 1998; **709**:289–295.
24 Kim TH, Park IK, Nah JW, Choi YJ, Cho CS. Galactosylated chitosan/DNA nanoparticles prepared using water-soluble chitosan as a gene carrier. *Biomaterials* 2004; **25**:3783–3792.
25 Chun CJ, Lee SM, Kim CW, Hong KY, Kim SY, Yang HK, *et al.* Doxorubicin-polyphosphazene conjugate hydrogels for locally controlled delivery of cancer therapeutics. *Biomaterials* 2009; **30**:4752–4762.
26 Virgolini I, Müller C, Klepetko W, Angelberger P, Bergmann H, O'Grady J, *et al.* Decreased hepatic function in patients with hepatoma or liver metastasis monitored by a hepatocyte specific galactosylated radioligand. *Br J Cancer* 1990; **61**:937–941.
27 Tomlinson R, Heller J, Brocchini S, Duncan R. Polyacetal-doxorubicin conjugates designed for pH-dependent degradation. *Bioconjug Chem* 2003; **14**:1096–1106.
28 Hovorka O, Šťastný M, Etrych T, Šubr V, Strohalmb J, Ulbrich K, *et al.* Differences in the intracellular fate of free and polymer-bound doxorubicin. *J Control Release* 2002; **80**:101–117.
29 Zhang C, Qu GW, Sun YJ, Wu XL, Yao Z, Guo QL, *et al.* Pharmacokinetics, biodistribution, efficacy and safety of N-octyl-O-sulfate chitosan micelles loaded with paclitaxel. *Biomaterials* 2008; **29**:1233–1241.
30 Fiume L, Baglioni M, Bolondi L, Farina C, Di Stefano G. Doxorubicin coupled to lactosaminated human albumin: a hepatocellular carcinoma targeted drug. *Drug Discov Today* 2008; **13**:1002–1009.
31 King HD, Staab AJ, Pham-Kaplita K, Yurgaitis D, Firestone RA, Laschb SJ, Trailb PA. BR96 conjugates of highly potent anthracyclines. *Bioorg Med Chem Lett* 2003; **13**:2119–2122.
32 Calderón M, Warnecke A, Gräser R, Haag R, Kratz F. Development of enzymatically cleavable doxorubicin conjugates with polyglycerol. *J Control Release* 2008; **132**:e54–e55.
33 Cui JX, Li CL, Guo WM, Li YH, Wang CX, Zhang L. Direct comparison of two pegylated liposomal doxorubicin formulations: is AUC predictive for toxicity and efficacy? *J Control Release* 2007; **118**:204–215.